

# Coherent dynamics in cavity femtochemistry: application of the multi-configuration time-dependent Hartree method.

Oriol Vendrell<sup>a,\*</sup>

<sup>a</sup>Department of Physics and Astronomy, Aarhus University, Ny Munkegade 120, 8000 Aarhus C, Denmark

---

## Abstract

The photochemistry of a molecular ensemble coupled to a resonance cavity and triggered by a femtosecond laser pulse is investigated from a real-time, quantum dynamics perspective with the multi-configuration time-dependent Hartree method. Coherent excitation of a superposition of electronic states in the ensemble leads to superradiant energy transfer to the cavity characterized by quadratic scaling with the number of molecules. Electronic decoherence associated with loss of nuclear wave packet overlap among those states destroys superradiant energy transfer, returning to a linear regime. For equal pump laser conditions, the photoexcitation probability per molecule decreases with increase of the number of molecules inside the cavity. This is caused by a loss of resonance condition of the laser with the bright electronic-photonic states of the coupled cavity-ensemble system. Increase of the laser bandwidth restores the energy transferred per molecule and the trigger probability remains independent of the number of molecules in the cavity.

*Keywords:* cavity electrodynamics, femtochemistry, superradiance, quantum dynamics

---

## 1. Introduction

The interaction of atoms [1–5] and ions [6] with quantized light has long been well known and investigated in depth. In recent years, interest for the fundamental properties and technological applications of hybrid light-matter systems of molecular nature is quickly raising, which is motivated to a large extent by the high tunability and relative ease of preparation of such systems [7–12]. From a *chemical* perspective, hybrid systems composed of a molecular ensemble coupled to a resonance cavity can lead to novel strategies to steer [8, 10, 12–17] and spectroscopically probe [18] the molecular properties and response of their individual members by exploiting their collective coupling to the cavity.

Recent theoretical investigations have elucidated cavity effects on the non-adiabatic molecular dynamics of a single coupled molecule [16, 19]. The effect on bonding and electronic structure parameters of molecules in a cavity has been as well the subject of recent investigations [14, 20–23]. As expected, such investigations confirm that structural properties such as bond length or orientation are, to a large extent, related to the individual coupling strength of each molecule to the cavity.

Specially interesting are theoretical proposals to exploit collective coupling effects as a way to alter the chemical evolution of the molecules in the cavity. These may involve either quenching [17] or enhancing [24] photochemical reactions in excited electronic states, in which the presence

of a molecular ensemble becomes important. In Ref. [17], for example, it was proposed that a photochemical reaction can be suppressed by the admixture of ground state character, which features a potential energy barrier, to some of the excited polaritonic (i.e. involving coupled electronic and photonic degrees of freedom) potential energy surfaces (PES), whereby an initial wavepacket was assumed to evolve on the lowest polaritonic PES after an instantaneous trigger process. In this respect, there is experimental evidence that, at least for reaction rates, the alteration of chemically relevant properties by a cavity is possible [10].

The quick increase in dimensionality of the Hilbert space when describing molecular-cavity problems involving a molecular ensemble has led to the application of different kinds of theory approaches. On the one hand, an adiabatic separation of nuclear and electronic and photonic degrees of freedom can be invoked, which leads to the construction of polaritonic PES. To obtain those, the polaritonic Hamiltonian parametrized by the nuclear positions is diagonalized, very often in the single molecular electronic excitation space, such that the rank of the Hamiltonian matrix grows linearly with the number of molecules  $N$  [17, 24, 25]. Therefore, such treatments have been able to account for situations with a low excitation density – i.e. a low number of cavity photons per molecule.

On the other hand, full quantum dynamics studies based on the standard method, meaning a product-grid representation of the wavefunction for all degrees of freedom, have been reported [14, 16, 19, 23]. These approaches naturally account for quantum evolution of nuclear, electronic and

---

\*Corresponding author

Email address: [oriol.vendrell@phys.au.dk](mailto:oriol.vendrell@phys.au.dk)

photonic degrees of freedom. They face, however, a dramatic exponential scaling when treating  $N$ -molecule ensembles in a cavity and therefore have been limited to the description of one [16, 19, 23] or two molecules [14] coupled to the electromagnetic modes.

The description of hybrid systems in terms of polaritonic PES has been recently extended to a surface-hopping algorithm for classical nuclear trajectories [26] to account for polaritonic transitions [25]. This opens interesting possibilities to follow the time evolution and relaxation of polaritons in a cavity for large molecular numbers, and for complex molecules. Nonetheless, theoretical descriptions based on classical mechanics for the nuclei are not able to account for the coherent quantum evolution among members of the molecular ensemble as prepared, e.g., by femtosecond pump lasers, and offer a limited description of electronic decoherence processes [27], which may be important at short times upon photo-excitation [28, 29].

For example, a challenging scenario is presented by the coherent excitation of *all* members of a molecular ensemble by a femtosecond laser pulse to produce, for each of the molecules, a superposition of two (or more) electronic states. This situation leaves the ensemble in a “cooperative” state, as termed by Dicke in his seminal work [30], which can lead to superradiant energy transfer to electromagnetic modes. States of this kind have been experimentally achieved recently for an ensemble of as many as  $10^{13}$  spins in a resonance cavity, which were shown to couple to the cavity mode in the superradiant regime [31]. The theoretical consideration of analogous situations with molecules requires the inclusion of the nuclear degrees of freedom besides accounting for the full space of polaritonic states with  $2^N$  molecular excitations, for  $N$  molecules and two electronic states per molecule.

In this work, full wavepacket quantum dynamics of an  $N$ -molecule ensemble coupled to a cavity and ranging from low to high excitation densities is considered and efficiently solved. Thereby, collective responses follow exclusively from the coupled dynamics of the separate constituents and no collective parameters, e.g., the Rabi splitting of the whole ensemble, enter the Hamiltonian. The theoretical description is free from the construction of polaritonic adiabatic PES (and their couplings) on which the nuclei evolve. Instead nuclear, electronic and photonic degrees of freedom are propagated quantum dynamically on the same footing for all members of the ensemble and the cavity. In this way, the models investigated explicitly consider the coupling of each molecule to the cavity and to external fields, e.g., femtosecond laser pulses pumping or driving the system.

This level of description is achieved by employing the highly efficient multi-configuration time-dependent Hartree (MCTDH) method for the propagation of multidimensional wavepackets [32–35]. As it will be discussed, the tensorial contraction of the wave function in the primitive grid basis representation inherent to MCTDH (and its multilayer extension) ideally suits the description of a

molecular ensemble coupled to a cavity, thus accounting for quantum correlations among the ensemble members and, if needed, for large photon numbers in the cavity.

This theoretical framework will be used to shed light on fundamental aspects of the interaction of the molecular ensemble with the cavity. In Sec. 3.2 the short time dynamics of the molecular ensemble under coherent excitation by femtosecond laser pulses will be described in detail. Section 3.3 analyzes the mechanism of coherent energy transfer between the ensemble and the cavity, and the role of electronic coherence, whereas Sec. 3.4 explores situations in which the number of photons in the cavity is similar or larger than the number of molecules in the ensemble. Before this, Sec. 2 lays down the theoretical framework for the description of ensemble-cavity systems and for the application of the MCTDH method to compute their quantum dynamical evolution.

## 2. Theoretical Framework and Computational Details

### 2.1. Molecular ensemble-cavity Hamiltonian

Our subject of investigation is an ensemble of molecules placed inside a cavity that supports quantized electromagnetic modes. The molecular density is assumed low enough that molecule-molecule interactions can be neglected [1, 2, 30]. Hence each molecule is coupled solely to the quantized electromagnetic modes of the cavity and to external electromagnetic radiation, – e.g. a laser pulse – which is described classically.

The basic form of the Hamiltonian for such scenario is well known and has been presented elsewhere [14, 16, 19, 23]. Here, the development of Ref. [23] is closely followed. Compared to other treatments, it keeps a quadratic dipole self-energy term [36] in the light-matter interaction (see below), which becomes only relevant in the ultra-strong coupling limit. In our case we keep this term for completeness but it has no effect on the dynamics for the range of conditions investigated.

Usually a Rabi-type term [37] describes the coupling of each molecule to the electromagnetic modes via a nuclear-position dependent dipole [14, 16, 23]. The Jaynes-Cummings [1] (and Tavis-Cummings for an ensemble [2]) Hamiltonian follows if one adopts the rotating wave approximation, employed e.g., in Refs. [15, 19, 25], but not in this work.

In the following, the Hamiltonian of the ensemble-cavity system is introduced with emphasis on the aspects relevant to this work. The Hamiltonian for the hybrid system is given by

$$\hat{H} = \sum_{l=1}^N \hat{H}_{\text{mol}}^{(l)} + \hat{H}_{\text{cav}} + \hat{H}_{\text{las}}, \quad (1)$$

where the Hamiltonian of the  $l$ -th molecule

$$\hat{H}_{\text{mol}}^{(l)} = \hat{T}_n^{(l)} + \hat{H}_e^{(l)} \quad (2)$$

is written as a sum of its nuclear kinetic energy  $\hat{T}_n^{(l)}$  and its clamped nuclei Hamiltonian  $\hat{H}_e^{(l)}$ , including the electronic kinetic energy and all intra-molecular Coulombic interactions [38]. The Hamiltonian of the quantized electromagnetic modes and their interaction with the molecules,

$$\hat{H}_{\text{cav}} = \frac{1}{2} \left[ \hat{p}^2 + \omega_c^2 \left( \hat{q} + \frac{\vec{\lambda} \cdot \hat{\vec{D}}}{\omega_c} \right)^2 \right], \quad (3)$$

is given in the harmonic oscillator form, in length gauge and in dipole approximation [16, 23]. Only one mode is considered for the sake of clarity.  $\omega_c$  is the angular frequency of the cavity mode and  $\vec{\lambda}$  is the dipole coupling strength  $\lambda = \sqrt{1/\epsilon_0 V}$  times the unit polarization vector in the given cavity.  $\hat{\vec{D}}$  is the dipole operator acting on all matter degrees of freedom and  $V$  is the volume of the quantized cavity mode. In Eq. (3) one can substitute  $\hat{q} = \sqrt{\hbar/2\omega_c}(\hat{a}^\dagger + \hat{a})$  and  $\hat{p} = i\sqrt{\hbar\omega_c/2}(\hat{a}^\dagger - \hat{a})$  and expand the quadratic term to reach [36]

$$\hat{H}_{\text{cav}} = \hbar\omega_c \left( \frac{1}{2} + \hat{a}^\dagger \hat{a} \right) + \sqrt{\frac{\hbar\omega_c}{2}} \vec{\lambda} \cdot \hat{\vec{D}} (\hat{a}^\dagger + \hat{a}) + \frac{1}{2} \left( \vec{\lambda} \cdot \hat{\vec{D}} \right)^2 \quad (4)$$

where  $\hat{a}^\dagger$  and  $\hat{a}$  are the photon creation and annihilation operators, respectively. The interaction with external fields, e.g., a femtosecond laser pulse, is treated semiclassically

$$\hat{H}_{\text{las}} = \vec{E}(t) \hat{\vec{D}}, \quad (5)$$

in the dipole approximation and in length gauge, where  $\vec{E}(t)$  is the time dependent electric field of the laser. The total dipole is simply the sum of the individual molecular dipoles

$$\hat{\vec{D}} = \sum_{l=1}^N \hat{\vec{D}}^{(l)}, \quad (6)$$

which in terms of the nuclear (uppercase) and electronic (lowercase) coordinates of each molecule read

$$\hat{\vec{D}}^{(l)} = q_e \left( \sum_{\alpha=1}^{N_n} Z_\alpha \vec{R}_\alpha^{(l)} - \sum_{\beta=1}^{N_e} \vec{r}_\beta^{(l)} \right) \quad (7)$$

with  $q_e$  the magnitude of the electron charge.

At this point, and without loss of generality, electronic adiabatic eigenstates  $|\psi_s^{(l)}(\mathbf{R}^{(l)})\rangle$  of the molecular clamped nuclei Hamiltonians  $\hat{H}_e^{(l)}$  are introduced

$$\hat{H}_e^{(l)} |\psi_s^{(l)}(\mathbf{R}^{(l)})\rangle = V_s^{(l)}(\mathbf{R}^{(l)}) |\psi_s^{(l)}(\mathbf{R}^{(l)})\rangle. \quad (8)$$

In the following, their parametric dependence on the nuclear coordinates  $(\mathbf{R}^{(l)})$  is dropped for the sake of clarity.

Projection of the  $l$ -th molecular Hamiltonian (2) onto the corresponding electronic basis

$$\hat{H}_{\text{mol}}^{(l)} \equiv \sum_{s=1}^{N_s} \sum_{r=1}^{N_s} |\psi_s^{(l)}\rangle \langle \psi_s^{(l)} | \hat{H}_{\text{mol}}^{(l)} | \psi_r^{(l)}\rangle \langle \psi_r^{(l)} | \quad (9)$$

introduces the matrix elements of the nuclear Hamiltonian

$$\begin{aligned} [\hat{H}_{\text{mol}}^{(l)}]_{sr} &= \langle \psi_s^{(l)} | \hat{H}_{\text{mol}}^{(l)} | \psi_r^{(l)} \rangle \\ &= \hat{T}_n^{(l)} + \hat{\Lambda}_{sr}^{(l)} + \hat{V}_s^{(l)} \delta_{sr}, \end{aligned} \quad (10)$$

in terms of adiabatic PES  $\hat{V}_s^{(l)}$  and their non-adiabatic couplings  $\hat{\Lambda}_{sr}^{(l)} = \langle \psi_s^{(l)} | \hat{T}_n^{(l)} | \psi_r^{(l)} \rangle - \hat{T}_n^{(l)} \delta_{sr}$  [38]. The brackets above denote integration over the electronic coordinates only. Similarly, projection of the dipole operator onto the same electronic basis yields

$$[\hat{\vec{D}}]_{sr}^{(l)} = \langle \psi_s^{(l)} | \hat{\vec{D}} | \psi_r^{(l)} \rangle = \hat{\mu}_{sr}^{(l)}(\mathbf{R}^{(l)}), \quad (11)$$

where  $\hat{\mu}_{sr}^{(l)}$  is the position dependent dipole (or transition dipole for  $s \neq r$ ) matrix element of the  $l$ -th molecule, obtainable, typically, from quantum chemistry calculations. No intermolecular dipole terms are considered in Eq. (11) because of the assumed zero overlap among electronic states of different molecules. (See discussion at the beginning of this section).

Throughout this work the molecules will be assumed to be aligned with the polarization axis of the cavity mode and of the external laser field, and the vector notation for the electric field and dipole operator will be dropped accordingly. The various parameters of the model that are relevant to each part of this investigation will be introduced as needed.

## 2.2. Quantum dynamics with MCTDH

The MCTDH method is an efficient approach to propagate the time-dependent Schrödinger equation for multi-dimensional systems. The method was first introduced to treat the multi-dimensional quantum dynamics of molecular systems [32, 39]. Over the years, though, applications to other types of problems, often linked to further developments of the basic theory, were successfully pushed forward, for example to describe the dynamics of electrons [40–42] and bosonic systems [43, 44], to name just a few. An in-depth review of the basic theory can be found in Ref. [34]. The quantum dynamics calculations in this work have been performed with the Heidelberg MCTDH package version v85.5 [45].

The basic theory is briefly described in this Section, where the usual nomenclature in the MCTDH literature is used for consistency [34]. The MCTDH ansatz specialized to the ensemble-cavity case is discussed in Sec. 2.3. The MCTDH ansatz for the wave function reads

$$\begin{aligned} |\Psi(q_1, \dots, q_f, t)\rangle &= \sum_{j_1}^{n_1} \dots \sum_{j_f}^{n_f} A_{j_1 \dots j_f}(t) \prod_{\kappa=1}^f |\varphi_{j_\kappa}^{(\kappa)}(q_\kappa, t)\rangle \\ &= \sum_J A_J(t) |\Phi_J(t)\rangle, \end{aligned} \quad (12)$$

where  $A_J(t)$  is the time-dependent expansion coefficient of the  $J$ -th configuration labeled with multi-index  $J$ , and  $|\Phi_J(t)\rangle$  is the  $J$ -th time-dependent Hartree product, which is a direct product of single-particle functions (SPFs) for each degree of freedom. These are analogous to molecular orbitals in electronic structure theory [46]. After applying a time-dependent variational principle to this ansatz the MCTDH equations of motion

$$i\dot{A}_J = \sum_L \langle \Phi_J | H | \Phi_L \rangle A_L, \quad (13)$$

$$i\dot{\varphi}^{(\kappa)} = (1 - P^{(\kappa)}) (\rho^{(\kappa)})^{-1} \langle \mathbf{H} \rangle^{(\kappa)} \varphi^{(\kappa)}$$

are obtained. Here a vector notation  $\varphi^{(\kappa)} = (|\varphi_1^{(\kappa)}\rangle, \dots, |\varphi_{n_\kappa}^{(\kappa)}\rangle)^T$  is used,

$$P^{(\kappa)} = \sum_{j=1}^{n_\kappa} |\varphi_j^{(\kappa)}\rangle \langle \varphi_j^{(\kappa)}| \quad (14)$$

is the projector on the space spanned by the SPFs for the  $\kappa$ th degree of freedom, and  $\langle \mathbf{H} \rangle^{(\kappa)}$  and  $\rho^{(\kappa)}$  are mean-fields and the density matrix [34].

The SPFs are expanded in turn in a time-independent basis for each degree of freedom

$$|\varphi_j^{(\kappa)}\rangle = \sum_{i=1}^{N_\kappa} c_{i,j}^{(\kappa)}(t) |\chi_i^{(\kappa)}\rangle, \quad (15)$$

where, for convenience, very often the states of the primitive representation  $|\chi_i^{(\kappa)}\rangle$  are taken from a discrete variable representation [34].

The efficiency gain in MCTDH compared to propagating directly in the primitive basis (the standard method) arises from the usually big difference between the size of the primitive space  $\prod_{\kappa=1}^f N_\kappa$ , and the size of the configuration space  $\prod_{\kappa=1}^f n_\kappa$  needed to achieve convergence in the correlated dynamics. Mode combination [35] (used here) and especially multilayer MCTDH [47–50], which is implemented in the Heidelberg MCTDH package [49], can boost even further the efficiency of the method allowing, in favorable cases, the description of hundreds to thousands of degrees of freedom [49, 51, 52].

### 2.3. MCTDH for the ensemble-cavity problem

Upon projection of the molecular Hamiltonians onto an electronic basis for each molecular system in (9), the total MCTDH wave function for the ensemble-cavity system molecules takes the form

$$|\Psi(t)\rangle = \sum_{j_1, \dots, j_N, j_p}^{n_1, \dots, n_N, n_p} A_{j_1, \dots, j_N, j_p}(t) \prod_{l=1}^N \left( \sum_{s_l=1}^{N_s} \phi_{s_l, j_l}^{(l)}(t) |\psi_{s_l}^{(l)}\rangle \right) \left( \sum_{P=1}^{N_p} B_{P, j_p}(t) |P\rangle \right). \quad (16)$$

Here the  $n_l$  and  $n_p$  are the number of SPF basis for each molecule and for the cavity mode, respectively, where nuclear and electronic degrees of freedom are combined to

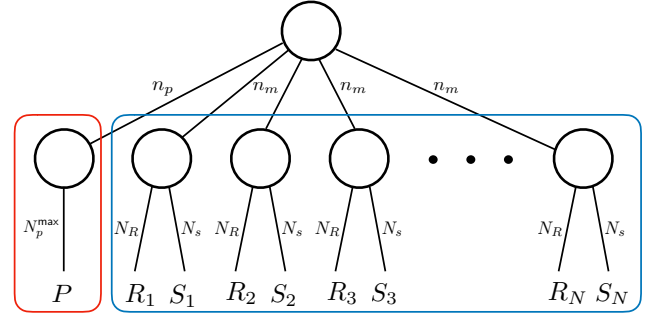


Figure 1: Tree representation of the MCTDH wave functions used to represent the cavity mode and the molecular ensemble. The red box marks the photonic mode and the blue box marks the molecular degrees of freedom.  $N_R$  and  $N_s$  refer to the number of primitive basis functions (grid points in this particular case) and number of electronic states in each molecule, respectively. The number of single particle functions for the molecules and for the cavity mode are  $n_m$  and  $n_p$ , respectively.  $P$ ,  $R_l$  and  $S_l$  denote the cavity, nuclear and electronic degrees of freedom, respectively.

one logical mode (cf. Fig. 1). As before,  $N_s$  is the number of relevant electronic states per molecule and  $N_p$  is the maximum number of photons allowed in the cavity. The  $\phi_{s_l, j_l}^{(l)}(t)$  functions are the nuclear wave packets for molecule  $l$  in electronic state  $s_l$ , whereby index  $j_l$  refers to the configuration space as specified by  $A_{j_1, \dots, j_N, j_p}$  in Eq. (16).  $B_{P, j_p}(t)$  are the expansion coefficients of the primitive photonic space for  $P$  cavity photons with configuration space index  $j_p$ . In absence of coupling between the molecules and the cavity, and of direct couplings between the molecules, one single Hartree product suffices in Eq. (16) and all  $\{n_l, n_p\}$  become equal to one.

Figure 1 presents a tree representation of the MCTDH wave function. Such representations become particularly useful to describe multilayer wave functions, but are also very illustrative in the normal (two layer) MCTDH case. The top node represents the  $A_{j_1, \dots, j_N, j_p}(t)$  tensor, with one line per index. The nodes at the bottom layer represent the expansion coefficients of the molecular functions  $\phi_{s_l, j_l}^{(l)}(t)$  and the  $B_{P, j_p}(t)$  coefficients of the cavity mode. The left-most box in Fig. 1 encloses the photonic degree of freedom. Since the quantized mode of the cavity is represented in its harmonic oscillator form, naturally a DVR constructed from harmonic oscillator eigenfunctions [34] is used to represent the photonic states. The size of the primitive basis  $N_p$  determines the maximum number of photons in the cavity mode and has been set to values between 10 and 60, depending on the details of the corresponding calculation. A substantially larger number of cavity photons or further cavity modes could be accommodated with ease if required.

The right-most box in Fig. 1 encloses the molecular degrees of freedom. In this application we focus on diatomic molecules with two electronic states each. The interatomic distance  $R_l$  is discretized using a Fourier basis, and the electronic degree of freedom  $S_l$  is truly discrete with pos-



sible values, in this particular example (see below), 0 and 1. As already mentioned, the two degrees of freedom are here combined into one logical mode per molecule. The  $R$  grids have 4096 points each, which are necessary to describe the dissociative dynamics of the NaI system (introduced below) and to represent the momentum achieved by the relatively heavy atoms. Therefore each molecule’s primitive representation consists of 8192 grid points. The number of SPFs per mode required for converged results varies, but  $n_\kappa$  about 5 provides converged results in most of the wave packet propagations presented below. Finally, in MCTDH jargon, each molecule is described in a single-set formulation [35], which is the only practical alternative when each molecule carries its own electronic state index.

In terms of computational effort and scalability of the approach, technical details of the largest calculations in this study are reported in Table 1 and correspond to either 5 or 8 molecular systems and one cavity mode, referred for brevity as calculations  $C_5$  and  $C_8$ , respectively.  $C_5$  is dominated by the number of SPF coefficients, where most of the propagation time is spent, whereas the array of  $A_J$  coefficients is still short relative to typical MCTDH applications. This is due to the large size of the primitive grid needed to describe the photodissociation of NaI.  $C_8$  is a more balanced case, with an  $A_J$  array of order  $10^5$  entries and almost equal propagation time spent in the coefficients and the SPFs. In usual applications, order  $10^6$   $A_J$  coefficients are manageable, whereas order  $10^7$  becomes hard to propagate. This means, for this particular investigation, that 9 to 10 molecules can be treated at a good level of accuracy. Clearly, standard method calculations on the corresponding primitive grids are impossible in the foreseeable future.

As already mentioned, the calculations reported here are based on the normal (2-layer) MCTDH approach. Going beyond this system size, both in terms of molecular complexity and molecular number, requires using the multilayer MCTDH algorithm [47–50]. The Heidelberg implementation of multilayer MCTDH [45] has been recently applied to describe the photophysics of naphthalene (48 D) and anthracene (66 D) molecules in full dimensionality [53], as well as models of light-harvesting-complexes with hundreds of modes [54]. This indicates that the extension to even larger ensembles of high-dimensional molecular systems than will be discussed here should be within reach and will be the subject of future work.

#### 2.4. Molecular model

Following recent theoretical investigations involving one molecule in a cavity [16], we will consider here an ensemble of NaI molecules. This system is well known in the femtochemistry literature and features a relatively simple and well understood dynamics upon photo-excitation to its first singlet excited electronic state. The potential energy surfaces and transition dipole matrix elements are shown in Fig. 2 and were calculated with the GAMESS-US [56] package at the complete active self-consistent field

	$N_\Psi$	$N_A$	$N_{\text{prim}}$	$t_{\text{CPU}}/N_{\text{fs}}[\text{s}]$
$C_5$	$2.26 \times 10^5$	$2.18 \times 10^4$	$4.06 \times 10^{20}$	$\approx 700$
$C_8$	$7.86 \times 10^5$	$5.24 \times 10^5$	$2.23 \times 10^{32}$	$\approx 2500$

Table 1: Wave function size and computational effort for two representative calculations  $C_n$ , where  $n$  indicates the number of molecules in the cavity.  $N_\Psi$  correspond to the total number of complex coefficients representing the wave functions,  $N_A$  is the size of the  $A$ -vector in Eq. 12 and  $N_{\text{prim}}$  is the size of the primitive direct product basis, i.e. the size of the corresponding standard wave function in a hypothetical numerically exact propagation on the full grid. The wall-clock time per propagated fs  $t_{\text{CPU}}/N_{\text{fs}}$  has been scaled to one single processor (Intel Xeon E5-2680 v4 @ 2.4 GHz). Actual calculations were performed using shared-memory parallelization with up to 28 processors [55].

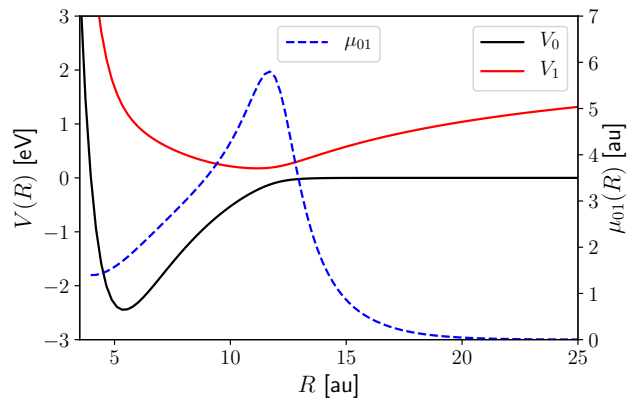


Figure 2: Potential energy curves of the ground  $V_0$  and first singlet excited  $V_1$  electronic states (solid curves) and transition dipole moment  $\mu_{01}$  along the molecular axis (dashed curve) for the NaI molecule obtained at the CASSCF level of theory (See main text for details).

(CASSCF) level of theory CAS(8,8), involving 8 valence orbitals (4 occupied, 4 virtual in the reference configuration) and 8 electrons. The inner valence and core electrons were treated with the SBKJC effective core potential [57].

It is not the goal of this investigation to obtain highly accurate potentials for NaI, and the level of electronic theory just described is sufficient for the purpose of this work. For example, the PES used in Ref. [16] feature a smaller gap between the two curves at the avoided crossing. While this gap affects non-adiabatic transitions within each member of the ensemble, these transitions are switched off in the present model with the purpose of highlighting the dynamical effects induced by the coupling to the cavity.

## 3. Results and Discussion

### 3.1. General considerations on the cavity-ensemble model

Throughout this work the effective cavity-matter coupling is taken as  $g/\omega_c=0.01$ , where  $g = \lambda\sqrt{\hbar\omega_c}/2$  is the rms vacuum electric field amplitude of the cavity mode [3] and  $\lambda$  was introduced around Eqs. (3)-(4). The use of  $g$

as the coupling strength parameter is in line with previous investigations [14, 16, 17] and facilitates direct comparisons. This coupling strength is small compared to the single-molecule ultra-strong coupling regime, characterized by a Rabi splitting of the polaritonic energy levels (at zero detuning)  $\hbar\omega_R = 2g\mu_{01}$  comparable to the transition energy. For the NaI molecule at the equilibrium geometry, the transition dipole  $\mu_{01}$  (cf. Fig 2b) is about 1.7 au, which results in  $\hbar\omega_R \approx 0.13$  eV. For more than one molecule, the collective Rabi splitting becomes  $\hbar\Omega_R = 2g\mu_{01}\sqrt{N}$  [58]. Hence for  $N = 5$  (calculations with up to  $N = 8$  were performed) the collective Rabi splitting at the Franck-Condon (FC) equilibrium geometry  $R_{\text{eq}}$  is of the order  $\hbar\Omega_R \approx 0.3$  eV, in line with earlier investigations [14, 16, 17].

In this work the cavity coupling  $g/\omega_c$  is kept *constant* for different numbers of molecules  $N$  (or molecular density  $N/V$ ) in the cavity. This is in contrast to other works where the collective Rabi splitting is kept constant by scaling the cavity coupling by  $1/\sqrt{N}$  [17, 24]. In the present context, Hamiltonian (1)-(7) describes the coupling of each individual member of the molecular ensemble to a *specific* cavity characterized by the quantization volume  $V$ , which is also the actual volume of the cavity. On the other hand, the Rabi splitting is a macroscopic quantity that emerges from the microscopic interactions. Under this consideration there is no *a priori* reason to fix  $\Omega_R$  for different number of molecules  $N$ . Therefore, our focus here will be on collective effects that emerge when varying  $N$  inside a given cavity, always in the limit of negligible direct interaction among ensemble members.

Concluding, we note that the coupling term between laser light and the hybrid system in Eq. 5 describes the interaction of the laser pulse with the molecules only. This is justifiable as long as the laser is non-resonant with the cavity frequencies. In situations, as discussed below, in which both the laser and the cavity are resonant with the Franck-Condon transition of the molecules, extra care with this assumption is required. It can, e.g., be conceived for the configuration in which the wave vectors  $\vec{k}_i$  of the electromagnetic modes of the laser lie parallel to the plane of the cavity mirrors (in a Fabry-Pérot configuration), such that the external laser field and the cavity modes share a common polarization axis [18]. On the other hand, direct coupling between the laser field and the cavity modes, for example in open plasmonic structures, may turn out to be the dominant coupling mechanism. From a computational perspective, the model discussed above may then be easily extended to include the corresponding laser-cavity coupling terms obtained either from phenomenological or first-principles considerations [59].

### 3.2. Femtosecond laser pump of a hybrid ensemble-cavity system

The excitation of a molecular ensemble with a short femtosecond laser pulse is considered first. The laser resonantly couples the ground and first excited electronic

states of each molecule, and the cavity is resonant as well with this electronic transition at the Franck-Condon geometry. The cavity and laser photon energy are both  $\hbar\omega_c = \hbar\omega_L = 3.8$  eV and the laser pulse is modelled as

$$E(t) = \sin^2\left(\frac{\pi t}{T_L}\right) \cos(\omega_L t), \quad (17)$$

where  $T_L$  is the total pulse duration and the full width at half maximum (FWHM) of the amplitude is  $\tau_L = T_L/2$ . Only the first period of the envelope function is considered and the pulse has zero amplitude at earlier and later times. The excitation by the short femtosecond pulse takes place in the impulsive regime: the relatively heavy nuclei of NaI practically do not move during the pulse duration. The most intense pulse considered corresponds to 0.003 au of peak field amplitude ( $3.16 \times 10^{11}$  W/cm<sup>2</sup>). This results in nearly a 50-50 superposition of the  $|\psi_0\rangle$  and  $|\psi_1\rangle$  electronic states for isolated molecules *without* a cavity, as illustrated in Fig. 3a. This pulse intensity is far from field-ionizing conditions at the optical frequencies considered here.

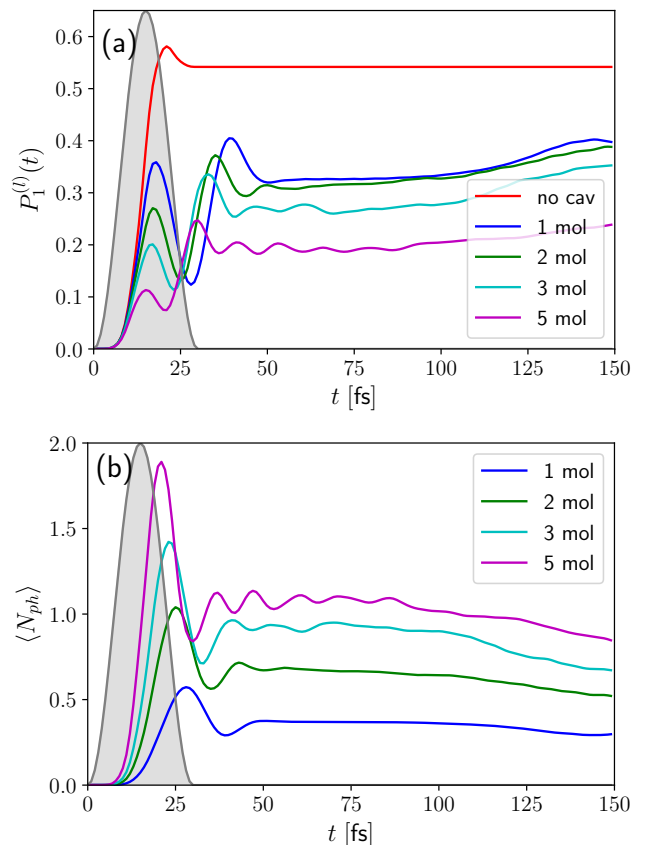


Figure 3: (a) Single molecule excited state population  $P_1^{(l)}(t) = |\langle \psi_1^{(l)} | \Psi(t) \rangle|^2$  and (b) expectation value of the cavity photon number  $\langle N_{ph} \rangle = \langle \Psi(t) | \hat{a}^\dagger \hat{a} | \Psi(t) \rangle$  as a function of time for propagations without a cavity and for 1 to 5 molecules in the cavity. The grey area indicates the envelope of the laser pulse (cf. Eq. (17)). The peak laser amplitude is 0.003 au (corresponding to  $3.16 \times 10^{11}$  W/cm<sup>2</sup>) and the photon energy  $\hbar\omega_L = 3.8$  eV.

The quantities of interest are the single molecule excited state population

$$P_1^{(l)}(t) = |\langle \psi_1^{(l)} | \Psi(t) \rangle|^2 \quad (18)$$

and the expectation value of the cavity photon number

$$\langle N_{ph} \rangle(t) = \langle \Psi(t) | \hat{a}^\dagger \hat{a} | \Psi(t) \rangle. \quad (19)$$

For more than one molecule in the cavity the molecular index  $l$  in Eq. (18) can take any value as all molecules are identical. For all molecule number cases considered, Fig. 3a shows a fast increase of the molecular excitation  $P_1^{(l)}(t)$  while the pulse intensity is still rising, but the presence of the cavity has a dramatic effect on how the pulse energy is redistributed in the system. Shortly after the molecular excitation probability peaks, the cavity mean photon number  $\langle N_{ph} \rangle$  starts increasing as the molecules transfer energy to the cavity in the onset of the first Rabi cycle. The number of molecules modulates the amplitude of the oscillations, as well as their period, as seen in Fig. 3b. This ongoing Rabi dynamics is of course a consequence of the coherent wave packet prepared by the laser pulse.

For the case of  $N = 5$ , characterized by the largest collective coupling of the ensemble and the cavity, an almost direct energy transfer from the laser pulse to the cavity mode takes place. The population of molecular excitations, which mediate the energy transfer to the cavity, remain very low during the duration of the laser pulse, which is reminiscent of a Stimulated Raman Adiabatic Passage (STIRAP)-type mechanism [60]. These dynamics correspond to a regime dominated by coherent time evolution among the polaritonic states impulsively populated by the short laser pulse. The time evolution of these oscillations roughly corresponds to  $\cos(\Omega_{\text{Rabi}}t)$ , which would be exactly the case in the simpler scenario of two-level atoms coupled to the same cavity and external field.

Nuclear motion, however, quickly quenches these dynamics by destroying the necessary electronic-photonic coherence. To see this, one can argue qualitatively for a moment in terms of a simple system with electronic  $s = \{0, 1\}$  and cavity photon  $P = \{0, 1\}$  degrees of freedom and an additional nuclear coordinate  $R$ . Before the onset of nuclear displacements the state of the system prepared by the laser can be written as

$$|\Psi(t)\rangle = \phi(R) \left( c_{01}(t) |\psi_0\rangle |1\rangle + c_{10}(t) |\psi_1\rangle |0\rangle \right) \quad (20)$$

where the off-diagonal coupling between both states is  $g\mu_{01}(R)$  (cf. also Eq. (A.1)) and the evolution of the photon number in the cavity given by

$$\langle N_{ph} \rangle = |c_{01}(t)|^2 \approx \sin^2(g\mu_{01}(R_{\text{eq}})t/\hbar). \quad (21)$$

After the nuclear wave packet in the excited electronic state leaves the FC region the state of the system can qualitatively be written as

$$|\Psi(t)\rangle = c_{01}(t) \phi_0(R, t) |\psi_0\rangle |1\rangle + c_{10}(t) \phi_1(R, t) |\psi_1\rangle |0\rangle, \quad (22)$$

where the nuclear wave packet evolves differently in the two molecular electronic states and where both  $\phi_s(R, t)$  are normalized. Now, as the nuclear wave packet  $\phi_1(R, t)$  in the excited electronic state becomes non-resonant with the cavity mode, the coupling to the cavity vanishes and  $|c_{01}(t)|$  becomes almost constant. The large oscillations in photon number stop. However, the  $\phi_0(R, t) |\psi_0\rangle |1\rangle$  component corresponds to the nuclei still at the FC region ( $R \approx R_{\text{eq}}$ ) with one cavity photon. Therefore, the cavity keeps promoting the molecular system from its ground to its excited electronic state, where it dissociates and cannot emit a photon back to the cavity. These dynamics continue until the cavity is completely relaxed. The onset of this dynamical regime is indeed seen in the MCTDH numerical results in Fig. 3b for all molecular numbers as a continuous decrease in photon number that starts at 40 to 50 fs and has its counterpart in an increase of the excitation probability per molecule in Fig. 3a.

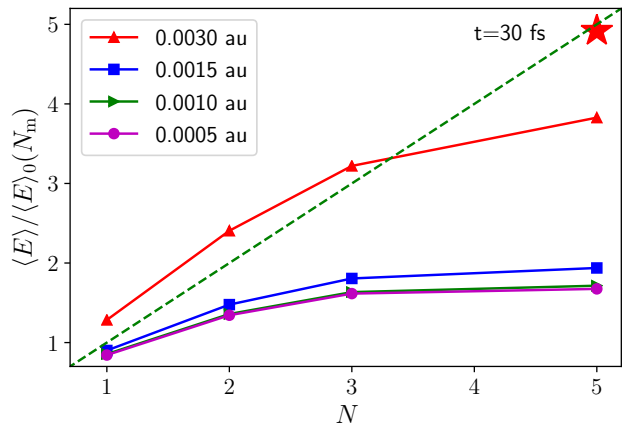


Figure 4: Energy transfer to the hybrid ensemble-cavity system relative to the energy transfer to a single isolated molecule for different molecule numbers and laser peak intensities after the laser pulse is over. The laser pulse has the intensity profile shown in Fig. 3 except for the simulation with 5 molecules and marked with a red star, in which the pulse energy is preserved but the FWHM of the intensity profile is shortened by a factor of 3 to increase the laser bandwidth.

We just discussed how the onset of nuclear motion strongly modifies and quenches the coherent polaritonic dynamics that a femtosecond laser imprints onto the hybrid system. We see as well that  $P_1^{(l)}(t)$  in Fig. 3a reaches a smaller value after the pulse for  $N = 5$  as compared to  $N = 1$ . Although  $\langle N_{ph} \rangle$  in Fig. 3b grows faster and reaches a larger value after the pulse for  $N = 5$  molecules, this does not compensate for the much lower molecular excitation. Indeed, the total amount of energy *per molecule* transferred by the external laser to the system is decreasing with the number of molecules, as illustrated in Fig. 4 for different laser intensities. This figure presents the ratio between the total energy transferred to the hybrid system by the laser pulse and the total energy transferred to a single molecule with no cavity, also after the pulse. The

results in Fig. 4 illustrate how, for increasing number of molecules and equal laser conditions, the relative likelihood that one of the molecules is photoexcited and is able to start a photochemical process decreases, which is reminiscent of the findings in Ref. [17].

To understand the origin of this trend we note that the collective Rabi splitting at the FC point reaches a value  $\Omega_R \approx 0.3$  eV for  $N = 5$ , whereas a pulse duration 15 fs FWHM corresponds to a bandwidth of about 0.27 eV. Therefore, as the number of molecules increases, the upper and lower polaritonic states of the hybrid system drift out of resonance with the laser pulse. To demonstrate that energy transfer to the coupled ensemble is determined by the bandwidth of the femtosecond pulse, a simulation with a shorter pulse of duration  $\tau_S = \tau_L/3$  and  $N = 5$  is made. The maximum field amplitude is scaled by a factor  $\sqrt{3}$  to maintain the area under the intensity envelope of the two pulses exactly constant, therefore achieving the same pulse energy. The pulse bandwidth increases now to about 0.8 eV. The final energy ratio for this simulation is shown with a star in Fig. 4 and falls almost exactly on the linear trend as a function of the number of molecules. It is emphasized that the denominator  $\langle E \rangle_0$  is the same for the long and short pulse simulations, namely the energy transferred by the longer pulse to a single isolated molecule.

Therefore, if the pump laser pulse is sufficiently short to cover with its bandwidth the splitted polaritonic states in the cavity, the energy transferred per molecule becomes the same as for a single isolated molecule with that same laser. From a purely time-dependent perspective, once the pump laser is significantly shorter than the Rabi period, the molecules in the cavity become excited by the laser before being able to interact with the cavity and during these initial moments it is as if the cavity would not be present.

A consequence of this is that the probability for the photochemical process in the excited electronic state to take place becomes independent of the number of molecules in the cavity. This last point is further illustrated in Fig. 5, where the probability density  $\rho(R_t)$  for the nuclear degrees of freedom is shown at  $t = 100$  fs. For one single molecule in the cavity, the area under the curve at the right side of the coordinate for the dissociating systems is essentially the same as for one molecule without a cavity, whereas it is strongly suppressed for 5 molecules, as seen in Fig. 5b, due to the lower level of excitation per molecule. Figure 5b also illustrates, however, how the propagation initiated with a larger laser bandwidth restores the dissociation probability.

This last point contrasts with Ref. [17], where the photochemical reaction likelihood was found to decrease with increased number of molecules in a cavity. There, the trigger process was not considered and the molecules were directly promoted to the lower adiabatic polaritonic PES. To shed light on those aspects, two further calculations using the longer laser pulse with photon energy shifted by  $\pm 0.2$  eV are considered. These target, respectively, the

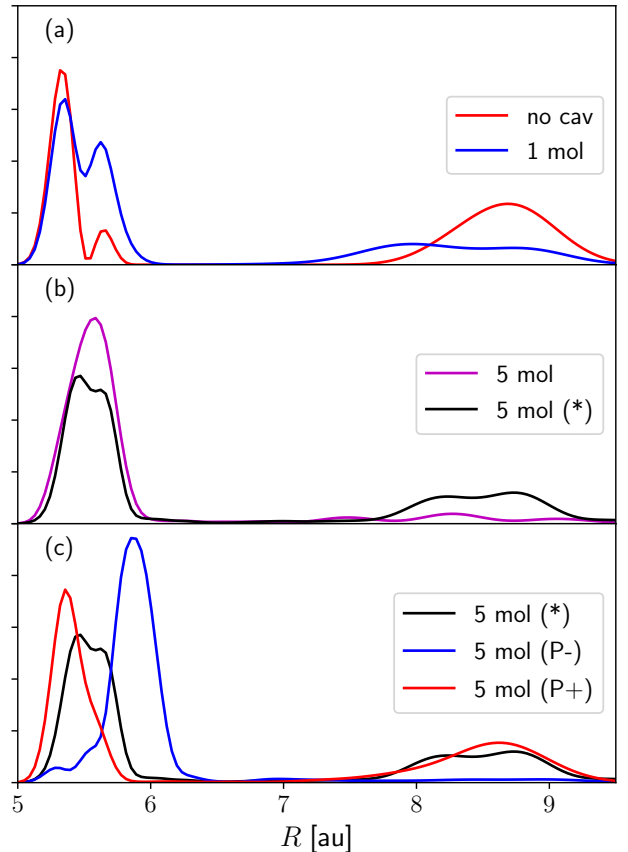


Figure 5: Probability density  $\rho(R_t)$  for the nuclear degrees of freedom at  $t = 100$  fs for the same laser conditions as in Fig. 3. (a) no cavity and one molecule in the cavity. (b) 5 molecules in the cavity. (\*) indicates an increased laser bandwidth. (c) 5 molecules in the cavity. (\*) as in (b). ( $P-$ ) and  $P(+)$  indicate laser tuned to the lower and higher polariton branches, respectively. (see text for details).

lower and upper polariton branches. As the laser is tuned to the lower branch, indicated as ( $P-$ ) in Fig. 5c, the reaction is almost completely suppressed. However, the energy transfer to the hybrid system relative to a single molecule is now  $\langle E \rangle / \langle E_0 \rangle = 7.28$  (cf. Fig. 4), even larger than the value of  $\approx 5$  corresponding to a broadband, shorter excitation and signaled with a red star in Fig. 4. So, even if a higher excitation density is achieved by tuning to the lower polariton, presumably the large admixture of ground electronic state character in the lower branch-states suppresses the start of the photochemical process, in line with the findings in Ref. [17].

On the other hand, as seen in Fig. 5c, when the laser is tuned to the upper polariton branch, the opposite effect is achieved and the photodissociation of each ensemble member is enhanced to the level of the isolated molecule case, which is explained by the enhanced excited electronic state character of the upper polaritonic branch. Therefore, a description of the pump process and of the initially prepared state are in general crucial elements to predict the reaction mechanisms in the coupled ensemble-cavity system.



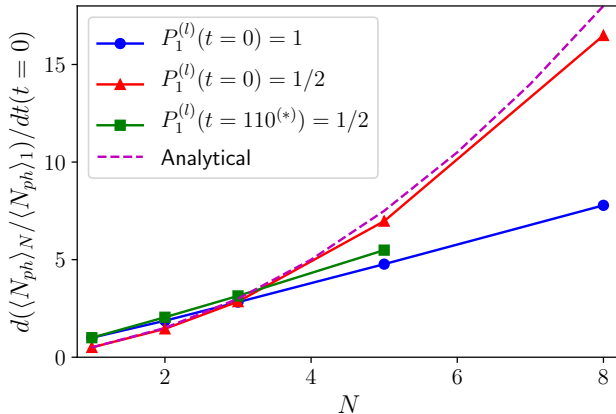


Figure 6: Relative energy transfer rate to the cavity mode relative to the single molecule case. All molecules excited with probability one (blue circles) and all molecules excited with probability 1/2 to the excited state (red triangles), immediately after excitation and for a cavity resonant with the FC transition energy. Relative rate of energy transfer for excited molecules in the  $V_1$  PES at  $t = 110$  fs, as they become resonant with a cavity  $\omega_c = 1$  eV (green squares). The analytical curve corresponds to the term in parenthesis in Eq. (24) for  $p_0 = p_1 = 1/2$  and  $S_{01} = 1$ .

### 3.3. Superradiant energy transfer to the cavity

As discussed before, a short femtosecond pulse imprints a coherent excitation on the coupled ensemble-cavity system. We now focus on the coherent dynamical evolution of the coupled system and the participation of the cavity mode in the dynamics of the individual molecules. The cavity is still tuned to be resonant at the FC geometry, and it is assumed that the molecules have been coherently excited by a laser pulse substantially shorter than their collective Rabi period in the cavity. The initial state at  $t = 0$  thus reads

$$|\Psi(0)\rangle = \prod_{l=1}^N \left( \sqrt{p_0} \phi_0^{(l)}(R_l) |\psi_0^{(l)}\rangle + \sqrt{p_1} \phi_1^{(l)}(R_l) |\psi_1^{(l)}\rangle \right) |0\rangle \quad (23)$$

where the same definitions as in Eq. (16) are used.  $\phi_s^{(l)}(R_l)$  is the nuclear wavepacket evolving on the PES of electronic state  $|\psi_s^{(l)}\rangle$ , and  $p_s$  is the initial electronic population of this state. In contrast to Eq. (16), the norm of the nuclear wave packets, which is the population of the corresponding electronic state, has been singled out for the sake of clarity, and hence the  $\phi_s^{(l)}(R_l)$  are assumed normalized. Equation (23) is a single Hartree product of the form of Eq. (16) and corresponds to the ground state of the complete system for  $p_1 = 0$ .

The total energy transferred from the molecules to the cavity at time  $t$  is proportional to the number of cavity photons  $\langle N_{ph} \rangle(t)$ . In second order in time the number of cavity photons is given by

$$\langle N_{ph} \rangle(t) = t^2 \mu_{01}^2 g^2 \left( N p_1 + (N^2 - N) p_0 p_1 |S_{01}|^2 \right), \quad (24)$$

where the nuclear overlap  $S_{01} = \langle \phi_0^{(l)} | \phi_1^{(l)} \rangle$  is 1 at short times for a FC transition. The molecular index drops from  $S_{01}$  because all molecules are assumed to be identical. The justification of Eq. (24) is given in the Appendix. It is interesting to note that, if the nuclear overlap is set to one as for atomic radiators, the term in parenthesis in Eq. (24) is the same as the linear (in time) radiation rate for an ensemble of coherently excited radiators coupled to an electromagnetic mode, which was first described by Dicke and termed superradiance [30]. The quadratic scaling with time in Eq. (24) is a natural consequence of Schrödinger's equation at short times and is of no particular interest. We are interested, instead, in the scaling with the molecular number  $N$ , which varies from linear to quadratic and which, as mentioned, is found in identical form in Dicke's radiation rate derived using Fermi's golden rule.

When all molecules are promoted to their corresponding state  $|\psi_1\rangle$  with probability  $p_1 = 1$  the energy transfer to the cavity grows linearly with the number of molecules, as predicted by Eq. (24) and numerically shown in Fig. 6. In contrast, when molecules are promoted to a coherent superposition of the ground and excited electronic states with  $p_0 = p_1 = 1/2$  the energy transfer to the cavity scales quadratically with  $N$ . However, as the nuclear overlap drops to zero, the coherent quadratic contribution disappears and the scaling becomes linear in  $N$  again. The latter regime is illustrated in Fig. 7 for the case in which the cavity is resonant with the molecules outside the vicinity of the FC point. In this set of calculations the cavity is resonant with a potential energy gap of 1 eV, which is reached by the molecules roughly 110 fs after photoexcitation. The population transfer *per molecule* back to the ground electronic state at  $t \approx 110$  fs is practically independent of  $N$ , and the number of cavity photons  $\langle N_{ph} \rangle$  (not shown) after the molecules have passed by the interaction region is just proportional to  $N$ . This is illustrated with the square marks in Fig. 6. The return to a linear scaling for the energy transfer to the cavity with  $N$  outside the FC region is hence the consequence of the loss of wave packet overlap between wave packets evolving on different PES of the same molecule, which effectively results in electronic decoherence.

Indeed, a simplified expression for the off diagonal element of the reduced electronic density matrix of the  $l$ -th molecule can be derived from Eq. (23) assuming that the time-evolved wave packet retains a product structure

$$\begin{aligned} \rho_{01}^{(l)}(t) &= \langle \Psi(t) | \psi_0 \rangle \langle \psi_1 | \Psi(t) \rangle \\ &= \langle \phi_0^{(l)}(R_l, t) | \phi_1^{(l)}(R_l, t) \rangle \sqrt{p_0} \sqrt{p_1} \\ &= S_{01} \sqrt{p_0} \sqrt{p_1}. \end{aligned} \quad (25)$$

This expression is valid at short times and the molecular index has again disappeared in the last line because all molecules are considered identical. Comparison of Eqs. (24) and (25) shows that the loss of electronic quantum coherence at the single molecule level destroys super-

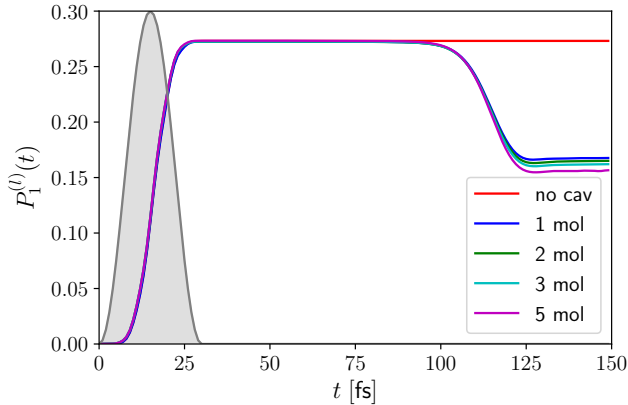


Figure 7: Single molecule excited state population  $P_1(t)$  for one isolated molecule and up to 5 molecules in the cavity. The pump laser intensity profile is shown in grey. The photon energy of the cavity mode is  $\hbar\omega_c = 1$  eV and is resonant with the molecules at an internuclear distance  $R \approx 10$  au.

radiant energy transfer to the cavity. In the case of NaI, with a dissociative excited PES,  $\rho_{01}^{(l)}(t) = 0$  for  $t > 0$  because of the loss of nuclear wavepacket overlap in the second line of Eq. (25). A more involved expression for  $\rho_{01}^{(l)}(t)$  can be obtained from the general ansatz (16), which however does not add any new physical insight to the conclusions reached from Eq. (25).

### 3.4. Stimulated emission by the cavity

The scenario in which the cavity becomes resonant with the molecular system along a reaction coordinate may be used to steer or probe photochemical reactions in ways analogous to the action of a laser pulse delayed with respect to the reaction trigger. When a photoexcited molecule reaches resonant configurations with the cavity, the cavity can stimulate the emission of one photon and dump the molecular system to the ground electronic state, as shown in Fig. 7, and which is part of the molecular relaxation mechanism discussed in [24]. An obvious control knob in a cavity is presented by its excitation level, the number of photons in the cavity, since the coupling term proportional to  $(\hat{a}^\dagger + \hat{a})$  in Eq. (4) effectively scales with  $\sqrt{N_{ph}}$  when applied to cavity state  $|N_{ph}\rangle$ . The excited electronic state population for one and five molecules interacting with a cavity is shown in Fig. 8 for different numbers of photons ranging from 0 to 30. The molecules are initially prepared in their excited electronic state with unit probability and the cavity's photon energy is  $\hbar\omega_c = 1$  eV.

The stimulated emission down to the ground electronic state strongly depends on the initial photon number of the cavity. After going through a maximum population dump for 5 to 10 photons, stimulated emission becomes indeed less efficient for 30 photons. The time evolution becomes non-trivial with a first plateau and a final complete dump, which is indicative of dynamics that proceed on effective potential surfaces strongly modified by the cavity coupling.

We compare now the cases with one and five molecules

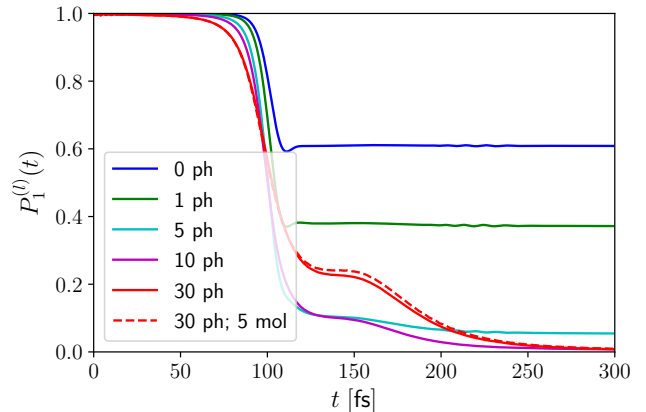


Figure 8: Single molecule excited state population  $P_1(t)$  as a function of time. The cavity mode has photon energy  $\hbar\omega_c = 1$  eV and various initial photon numbers are considered. All curves correspond to one single molecule in the cavity except for the curve (dashed red) corresponding to 30 photons and 5 molecules.

evolving in the cavity pre-loaded with 30 photons. It is found that the electronic population dynamics of each single molecule in the 5-molecule ensemble is essentially the same as the population dynamics of the single molecule case, as seen by comparing the two red curves in Fig. 8. An important difference is that the final state of the cavity (not shown) in the latter case corresponds to  $\langle N_{ph} \rangle = 35$  and in the former case to  $\langle N_{ph} \rangle = 31$ .

Comparing the probability density  $\rho(R, t)$  in Fig. 9 for either one or five molecules in the cavity, and after the passage through the resonant region at  $t = 200$  fs, two different regimes are seen: first, the wave packet splits between excited and ground state components for 0 and 1 photons in the cavity. Second, the wave packet is almost completely dumped to the ground state and remains uni-modal for 5 photons and beyond. Also for the nuclear evolution, the difference between one and five molecules in the cavity becomes insignificant (cf. Fig. 9f). For a high number of photons, which increases the effective molecule-cavity coupling, the nuclear wave packet becomes slowed down and partially trapped in the region in which the molecular electronic energy gap becomes resonant with the cavity. This effect has been seen in simulations with one photon but higher coupling strengths [14, 16].

The comparison between one and five molecules with 30 cavity photons is in line with the discussion in Sec. 3.3. As the excited molecules reach the interaction region there is no nuclear overlap and hence, as indicated in Eq. (24), the energy transfer to the cavity occurs linearly with the number of molecules, i.e. each molecule behaves as if it were alone in the cavity. Hence, the extent and rate of stimulated emission induced by a cavity resonant with the molecules along some photochemical reaction pathway is much more dependent on  $\langle N_{ph} \rangle$ , which determines the individual coupling of each molecule to the cavity, than the

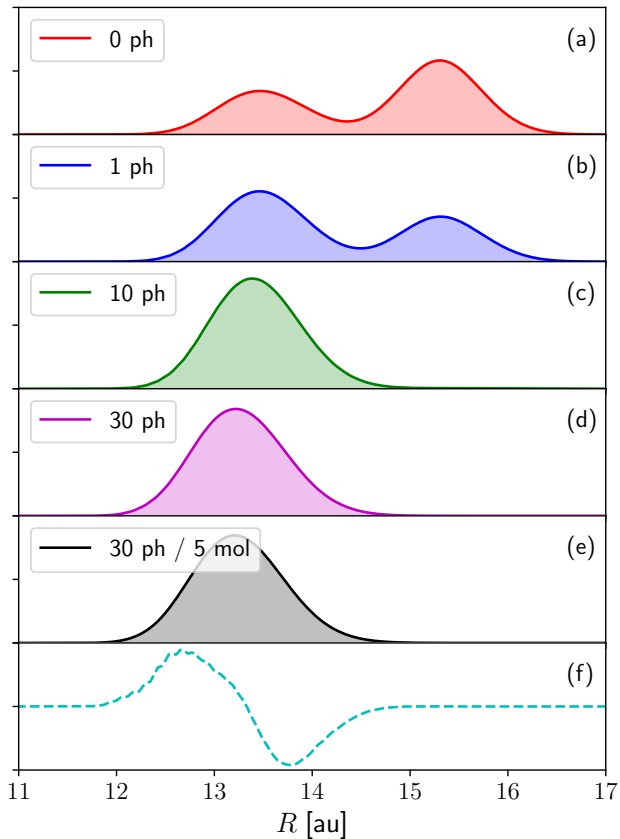


Figure 9: (a-e) One dimensional probability density  $\rho(R, t)$  for  $t = 200$  fs for the same simulations as shown in Fig. 8. (f) Probability density difference between cases (e) and (d) magnified  $\times 25$ .

molecular number (or density), which determines the total Rabi splitting but has a much smaller effect on the individual dynamics of the ensemble members. Moreover, even if a coherent superposition of molecular electronic states would be present, the number of photons in the cavity cannot be used to alter coherent effects that scale with  $N^2$ , as discussed in the Appendix around Eq. A.6.

#### 4. Summary and Conclusions

The real-time dynamics of an ensemble of molecules coupled to an electromagnetic cavity mode and pumped by a short femtosecond laser pulse was described by quantum wave packet simulations. In doing so, all coordinates of the microscopic Hamiltonian of the hybrid system were dynamically considered without resorting to an adiabatic separation in terms of polaritonic potentials and their couplings.

For a laser pulse with a duration FWHM of 15 fs, of order of the collective Rabi period of the hybrid system, the short time impulsive dynamics is triggered by the laser. These dynamics consist of Rabi oscillations in which the overall excitation oscillates between the molecules and the cavity. Nuclear motion of the excited molecules leads to

electronic-photonic decoherence among polaritonic states due to loss of nuclear wave packet overlap and quickly quenches these dynamics.

For the same laser conditions, the increase in the number of molecules (or the molecular density) leads to a decrease of the energy *per molecule* pumped to the cavity by the laser pulse, with the corresponding reduction of the probability per molecule that the photochemical reaction is started. It is found that this effect is caused by the laser drifting out of resonance with the bright polaritonic states as the collective Rabi splitting increases with the number of molecules. Increase of the laser bandwidth above the Rabi splitting *for the same pulse energy* restores the total energy transferred to linear scaling with the number of molecules, and restores the probability that the photochemical reaction is triggered by the femtosecond laser pulse. Alternatively, tuning the laser to the lower polariton branch leads to a suppression of the photochemical process due to the admixture of ground state character of such states, in line with Ref. [17].

When all molecules are coherently excited to a superposition of their ground and excited states, the energy transfer to the cavity occurs in a superradiant regime with quadratic scaling with the number of molecules. Again, this regime is destroyed by the loss of nuclear wave packet overlap within each individual molecule for the involved electronic states. This also means that the probability of photon emission to the cavity mode scales linearly with the number of molecules when the photoexcited molecules arrive at geometries resonant with the cavity along some reaction coordinate. The number of photons in the cavity has a very noticeable effect in stimulating emission to the cavity, but cannot be used to alter the dynamics related to coherent superposition of molecular electronic states.

In this application we chose NaI as a well known molecular system that has been the subject of numerous investigations, both experimental and theoretical, in the field of femtochemistry, and which undergoes a simple photodissociation process upon light absorption. This allowed us to concentrate on aspects of the excitation process and energy transfer dynamics in the cavity. By combining the same basic principles of this work with the multilayer MCTDH method, the study of a larger number of (multi-dimensional) molecules in a cavity, including possibly local dissipative baths and, if required, a larger number of cavity modes, is well within reach and opens new avenues for the rigorous investigation of cavity femtochemistry problems.

#### 5. Acknowledgments

I am grateful to Prof. Lars B. Madsen for stimulating discussions and critical reading of this manuscript. I wish to dedicate this work to Prof. Hans-Dieter Meyer on occasion of his 70th birthday, and to thank him for his continued mentorship and inspiration.

## Appendix A. Coherent energy transfer to the cavity

We consider an ensemble of two-electronic-state molecular radiators in a coherent superposition of their ground and excited state at  $t_0 = 0$ , which is given by Eq. (23). Such collective excitation can be achieved by a resonant laser pulser significantly shorter than the collective Rabi cycling period of the ensemble.

The system's Hamiltonian has the general form of Eqs.(1-11), where an electronic basis has been introduced, the second order light-matter coupling is left out, and the rotating wave approximation is used for the light-matter interaction

$$\hat{H} = \sum_{l=1}^N \left[ \hat{T}_l \hat{\mathbf{1}}_l + |\psi_0^{(l)}\rangle \hat{V}_0 \langle \psi_0^{(l)}| + |\psi_1^{(l)}\rangle \hat{V}_1 \langle \psi_1^{(l)}| \right. \quad (\text{A.1}) \\ \left. + \mu_{01} g \left( \hat{a}^\dagger |\psi_0^{(l)}\rangle \langle \psi_1^{(l)}| + \hat{a} |\psi_1^{(l)}\rangle \langle \psi_0^{(l)}| \right) \right] \\ + \hbar \omega_c \left( \frac{1}{2} + \hat{a}^\dagger \hat{a} \right).$$

As discussed in the main text,  $\mu_{01}$  is the transition dipole matrix element in the electronic basis and  $g$  corresponds to the light-matter coupling constant in the given cavity. For the above Hamiltonian (A.1) and initial state (23), with initially zero cavity photons, the expectation value of the photon-number in the cavity

$$\langle N_{ph} \rangle(t) = \langle \Psi(0) | \hat{U}^\dagger(t) \hat{a}^\dagger \hat{a} \hat{U}(t) | \Psi(0) \rangle \quad (\text{A.2})$$

is calculated by introducing a second-order expansion of the propagator

$$\hat{U}(t) \approx 1 - i\hat{H}t - \frac{1}{2}\hat{H}^2t^2. \quad (\text{A.3})$$

After some manipulations this leads to

$$\langle N_{ph} \rangle(t) = t^2 \mu_{01}^2 g^2 \left( \sum_{l=1}^N p_1 \langle \phi_1^{(l)} | \phi_1^{(l)} \rangle \right. \quad (\text{A.4}) \\ \left. + \sum_{\substack{k,l=1 \\ k \neq l}}^N \langle \phi_1^{(k)} | \phi_0^{(k)} \rangle \langle \phi_0^{(l)} | \phi_1^{(l)} \rangle p_0 p_1 \right) \\ = t^2 \mu_{01}^2 g^2 \left( N p_1 + (N^2 - N) p_0 p_1 |S_{01}|^2 \right),$$

where the last line could be rewritten in terms of the off-diagonal entry of the molecular electronic reduced density matrix, using  $p_0 p_1 |S_{01}|^2 \equiv |\rho_{01}|^2$  from Eq. (25). In the last line, it is considered that all molecular systems are identical and therefore the nuclear wavepacket overlaps  $S_{01} = \langle \phi_1^{(l)} | \phi_0^{(l)} \rangle$  are independent of molecular index  $l$ . The term in parenthesis in Eq. (A.4) with nuclear overlap  $S_{01} = 1$  can be readily compared with the rate expressions by Dicke in Ref. [30], in particular Eq. (26) for the case  $p_1 = 1$  and with Eq. (27) for the case  $p_1 = p_0 = 1/2$ .

The same calculation for initial state

$$|\Psi(0)\rangle = \prod_{l=1}^N \left( \sqrt{p_0} \phi_0^{(l)}(R_l) |\psi_0^{(l)}\rangle \right. \quad (\text{A.5}) \\ \left. + \sqrt{p_1} \phi_1^{(l)}(R_l) |\psi_1^{(l)}\rangle \right) |P\rangle,$$

i.e., with  $P$  cavity photons already present at  $t = 0$ , generalizes to

$$\langle N_{ph} \rangle(t) = P + t^2 \mu_{01}^2 g^2 \left( N[(P+1)p_1 - Pp_0] \right. \quad (\text{A.6}) \\ \left. + (N^2 - N) p_0 p_1 |S_{01}|^2 \right).$$

An important consequence of this result is that coherent dynamical evolution of the molecular ensemble and the cavity mode, which depends on a coherent superposition of the molecular electronic states, is completely insensitive to the number of photons in the cavity mode. Superradiance is as such a spontaneous emission process. On the other hand, as expected, the number of cavity photons enhances absorption and stimulated emission processes.

## References

- [1] E. T. Jaynes, F. W. Cummings, [Comparison of quantum and semiclassical radiation theories with application to the beam maser](#), Proc. IEEE 51 (1963) 89–109. doi:10.1109/PROC.1963.1664. URL <https://doi.org/10.1109/2Fproc.1963.1664>
- [2] M. Tavis, F. Cummings, The exact solution of n two level systems interacting with a single mode, quantized radiation field, Phys. Lett. A 25 (1967) 714–715. doi:10.1016/0375-9601(67)90957-7.
- [3] S. Haroche, D. Kleppner, Cavity quantum electrodynamics, Phys. Today 42 (1989) 24–30. doi:10.1063/1.881201.
- [4] R. Miller, T. E. Northup, K. M. Birnbaum, A. Boca, A. D. Boozer, H. J. Kimble, Trapped atoms in cavity QED: coupling quantized light and matter, J. Phys. B: At Mol Opt Phys 38 (2005) S551–S565. doi:10.1088/0953-4075/38/9/007.
- [5] H. Walther, B. T. H. Varcoe, B.-G. Englert, T. Becker, [Cavity quantum electrodynamics](#), Rep. Prog. Phys. 69 (2006) 1325–1382. doi:10.1088/0034-4885/69/5/R02. URL <https://doi.org/10.1088/0034-4885/69/5/R02>
- [6] P. F. Henskind, A. Dantan, J. P. Marler, M. Albert, M. Drewsen, Realization of collective strong coupling with ion coulomb crystals in an optical cavity, Nat. Phys. 5 (2009) 494–498. doi:10.1038/nphys1302.
- [7] S. Kéna-Cohen, M. Davanço, S. R. Forrest, Strong exciton-photon coupling in an organic single crystal microcavity, Physical Review Letters 101 (11) (2008) 116401. doi:10.1103/physrevlett.101.116401.
- [8] T. Schwartz, J. A. Hutchison, C. Genet, T. W. Ebbesen, [Reversible Switching of Ultrastrong Light-Molecule Coupling](#), Phys. Rev. Lett. 106 (2011) 196405. doi:10.1103/PhysRevLett.106.196405. URL <http://link.aps.org/doi/10.1103/PhysRevLett.106.196405>
- [9] T. Schwartz, J. A. Hutchison, J. Léonard, C. Genet, S. Haacke, T. W. Ebbesen, Polariton Dynamics under Strong Light–Molecule Coupling 14 125–131. doi:10.1002/cphc.201200734.



- [10] J. A. Hutchison, T. Schwartz, C. Genet, E. Devaux, T. W. Ebbesen, **Modifying Chemical Landscapes by Coupling to Vacuum Fields**, *Angew. Chem. Int. Ed.* 124 (2012) 1624–1628. doi:10.1002/ange.201107033. URL <https://doi.org/10.1002/ange.201107033>
- [11] J. George, S. Wang, T. Chervy, A. Canaguier-Durand, G. Schaeffer, J.-M. Lehn, J. A. Hutchison, C. Genet, T. W. Ebbesen, Ultra-strong coupling of molecular materials: spectroscopy and dynamics, *Faraday Discuss.* 178 (2015) 281–294. doi:10.1039/C4FD00197D.
- [12] T. W. Ebbesen, Hybrid Light–Matter States in a Molecular and Material Science Perspective, *Acc. Chem. Res.* 49 (2016) 2403–2412. doi:10.1021/acs.accounts.6b00295.
- [13] G. Morigi, P. W. H. Pinkse, M. Kowalewski, R. de Vivie-Riedle, Cavity cooling of internal molecular motion, *Phys. Rev. Lett.* 99 (2007) 073001. doi:10.1103/physrevlett.99.073001.
- [14] J. Galego, F. J. Garcia-Vidal, J. Feist, **Cavity-Induced Modifications of Molecular Structure in the Strong-Coupling Regime**, *Phys. Rev. X* 5 (2015) 041022. doi:10.1103/PhysRevX.5.041022. URL <https://doi.org/10.1103/2Fphysrevx.5.041022>
- [15] F. Herrera, F. C. Spano, Cavity-Controlled Chemistry in Molecular Ensembles, *Phys. Rev. Lett.* 116 (2016) 238301. doi:10.1103/PhysRevLett.116.238301.
- [16] M. Kowalewski, K. Bennett, S. Mukamel, Cavity Femtochemistry: Manipulating Nonadiabatic Dynamics at Avoided Crossings, *J. Phys. Chem. Lett.* 7 (2016) 2050–2054. doi:10.1021/acs.jpcclett.6b00864.
- [17] J. Galego, F. J. Garcia-Vidal, J. Feist, **Suppressing photochemical reactions with quantized light fields**, *Nat. Commun.* 7 (2016) 13841. doi:10.1038/ncomms13841. URL <http://www.nature.com/ncomms/2016/161212/ncomms13841/full/ncomms13841.html>
- [18] F. Caruso, S. K. Saikin, E. Solano, S. F. Huelga, A. Aspuru-Guzik, M. B. Plenio, **Probing biological light-harvesting phenomena by optical cavities**, *Phys. Rev. B* 85 (2012) 125424. doi:10.1103/PhysRevB.85.125424. URL <https://doi.org/10.1103/2Fphysrevb.85.125424>
- [19] M. Kowalewski, K. Bennett, S. Mukamel, Non-adiabatic dynamics of molecules in optical cavities, *J. Chem. Phys.* 144 (2016) 054309. doi:10.1063/1.4941053.
- [20] I. V. Tokatly, Time-dependent density functional theory for many-electron systems interacting with cavity photons, *Phys. Rev. Lett.* 110 (2013) 233001. doi:10.1103/physrevlett.110.233001.
- [21] M. Ruggenthaler, J. Flick, C. Pellegrini, H. Appel, I. V. Tokatly, A. Rubio, Quantum-electrodynamical density-functional theory: Bridging quantum optics and electronic-structure theory, *Phys. Rev. A* 90 (2014) 012508. doi:10.1103/physreva.90.012508.
- [22] J. A. Ćwik, P. Kirton, S. De Liberato, J. Keeling, Excitonic spectral features in strongly coupled organic polaritons, *Phys. Rev. A* 93 (2016) 033840. doi:10.1103/PhysRevA.93.033840.
- [23] J. Flick, M. Ruggenthaler, H. Appel, A. Rubio, Atoms and molecules in cavities, from weak to strong coupling in quantum-electrodynamics (QED) chemistry, *Proc. Natl. Acad. Sci.* 114 (2017) 3026–3034. doi:10.1073/pnas.1615509114.
- [24] J. Galego, F. J. Garcia-Vidal, J. Feist, Many-molecule reaction triggered by a single photon in polaritonic chemistry, *Phys. Rev. Lett.* 119 (2017) 136001. doi:10.1103/physrevlett.119.136001.
- [25] H. L. Luk, J. Feist, J. J. Toppari, G. Groenhof, Multiscale molecular dynamics simulations of polaritonic chemistry, *J. Chem. Theory Comput.* 13 (2017) 4324–4335. doi:10.1021/acs.jctc.7b00388.
- [26] J. Tully, Molecular dynamics with electronic transitions, *J. Chem. Phys.* 93 (1990) 1061–1071. doi:10.1063/1.459170.
- [27] J. E. Subotnik, N. Shenoi, A new approach to decoherence and momentum rescaling in the surface hopping algorithm, *J. Chem. Phys.* 134 (2011) 024105. doi:10.1063/1.3506779.
- [28] C. Arnold, O. Vendrell, R. Santra, Electronic decoherence following photoionization: Full quantum-dynamical treatment of the influence of nuclear motion, *Phys. Rev. A* 95 (2017) 033425. doi:10.1103/physreva.95.033425.
- [29] M. Vacher, M. J. Bearpark, M. A. Robb, J. P. Malhado, Electron dynamics upon ionization of polyatomic molecules: Coupling to quantum nuclear motion and decoherence, *Phys. Rev. Lett.* 118 (2017) 083001. doi:10.1103/physrevlett.118.083001.
- [30] R. H. Dicke, Coherence in spontaneous radiation processes, *Phys. Rev.* 93 (1954) 99–110. doi:10.1103/physrev.93.99.
- [31] B. Rose, A. Tyryshkin, H. Riemann, N. Abrosimov, P. Becker, H.-J. Pohl, M. Thewalt, K. Itoh, S. Lyon, Coherent rabi dynamics of a superradiant spin ensemble in a microwave cavity, *Phys. Rev. X* 7 (2017) 031002. doi:10.1103/physrevx.7.031002.
- [32] H. D. Meyer, U. Manthe, L. S. Cederbaum, **The multiconfigurational time-dependent Hartree-approach**, *Chem. Phys. Lett.* 165 (1990) 73. doi:10.1016/0009-2614(90)87014-i. URL [https://doi.org/10.1016/0009-2614\(90\)87014-i](https://doi.org/10.1016/0009-2614(90)87014-i)
- [33] U. Manthe, H.-D. Meyer, L. S. Cederbaum, Wave-packet dynamics within the multiconfiguration Hartree framework: General aspects and application to NOCl, *J. Chem. Phys.* 97 (5) (1992) 3199–3213. doi:10.1063/1.463007.
- [34] M. H. Beck, A. Jäckle, G. A. Worth, H.-D. Meyer, **The multiconfiguration time-dependent Hartree method: A highly efficient algorithm for propagating wavepackets.**, *Phys. Rep.* 324 (2000) 1–105. doi:10.1016/S0370-1573(99)00047-2. URL <https://doi.org/10.1016/2Fs0370-1573%2899%2900047-2>
- [35] H.-D. Meyer, G. A. Worth, **Quantum molecular dynamics: Propagating wavepackets and density operators using the multiconfiguration time-dependent Hartree (MCTDH) method**, *Theor. Chem. Acc.* 109 (2003) 251–267. doi:10.1007/s00214-003-0439-1. URL <https://doi.org/10.1007/2Fs00214-003-0439-1>
- [36] F. H. M. Faisal, **Theory of Multiphoton Processes**, Springer US, 1987. doi:10.1007/978-1-4899-1977-9. URL <http://www.springer.com/us/book/9780306423178>
- [37] I. I. Rabi, Space quantization in a gyrating magnetic field, *Phys. Rev.* 51 (1937) 652–654. doi:10.1103/physrev.51.652.
- [38] G. A. Worth, L. S. Cederbaum, **BEYOND BORN-OPPENHEIMER: molecular dynamics through a conical intersection**, *Annu. Rev. Phys. Chem.* 55 (2004) 127–158. doi:10.1146/annurev.physchem.55.091602.094335. URL <http://doi.org/10.1146/2Fannurev.physchem.55.091602.094335>
- [39] U. Manthe, H.-D. Meyer, L. S. Cederbaum, Multiconfigurational time-dependent Hartree study of complex dynamics: Photodissociation of NO<sub>2</sub>, *J. Chem. Phys.* 97 (1992) 9062–9071.
- [40] J. Caillat, J. Zanghellini, M. Kitzler, O. Koch, W. Kreuzer, A. Scrinzi, Correlated multielectron systems in strong laser fields: A multiconfiguration time-dependent hartree-fock approach, *Phys. Rev. A* 71 (2005) 012712. doi:10.1103/physreva.71.012712.
- [41] D. J. Haxton, K. V. Lawler, C. W. McCurdy, Multiconfiguration time-dependent hartree-fock treatment of electronic and nuclear dynamics in diatomic molecules, *Phys. Rev. A* 83 (2011) 063416. doi:10.1103/physreva.83.063416.
- [42] H. Miyagi, L. B. Madsen, Time-dependent restricted-active-space self-consistent-field theory for laser-driven many-electron dynamics. II. extended formulation and numerical analysis, *Phys. Rev. A* 89 (2014) 063416. doi:10.1103/physreva.89.063416.
- [43] O. E. Alon, A. I. Streltsov, L. S. Cederbaum, Unified view on multiconfigurational time propagation for systems consisting of identical particles, *J. Chem. Phys.* 127 (2007) 154103. doi:10.1063/1.2771159.
- [44] O. E. Alon, A. I. Streltsov, L. S. Cederbaum, Multiconfigurational time-dependent hartree method for bosons: Many-body dynamics of bosonic systems, *Phys. Rev. A* 77 (2008) 033613. doi:10.1103/physreva.77.033613.
- [45] G. A. Worth, M. H. Beck, A. Jäckle, O. Vendrell, H.-D.

- Meyer, The MCTDH Package, Version 8.2, (2000). H.-D. Meyer, Version 8.3 (2002), Version 8.4 (2007). O. Vendrell and H.-D. Meyer Version 8.5 (2013). Version 8.5 contains the ML-MCTDH algorithm. Current versions: 8.4.12 and 8.5.5 (2016). See <http://mctdh.uni-hd.de/>.
- [46] A. Szabo, N. S. Ostlund, *Modern Quantum Chemistry*, Dover, New York, 1983.
- [47] H. Wang, M. Thoss, Multilayer formulation of the multiconfiguration time-dependent Hartree theory, *J. Chem. Phys.* 119 (2003) 1289–1299.
- [48] U. Manthe, A multilayer multiconfigurational time-dependent hartree approach for quantum dynamics on general potential energy surfaces, *J. Chem. Phys.* 128 (2008) 164116.
- [49] O. Vendrell, H.-D. Meyer, [Multilayer multiconfiguration time-dependent Hartree method: Implementation and applications to a Henon–Heiles Hamiltonian and to pyrazine](#), *J. Chem. Phys.* 134 (2011) 044135. doi:10.1063/1.3535541. URL <https://doi.org/10.1063/1.3535541>
- [50] L. Cao, S. Krönke, O. Vendrell, P. Schmelcher, [The multi-layer multi-configuration time-dependent Hartree method for bosons: Theory, implementation, and applications](#), *J. Chem. Phys.* 139 (2013) 134103. doi:10.1063/1.4821350. URL [http://jcp.aip.org/resource/1/jcpsa6/v139/i13/p134103\\_s1](http://jcp.aip.org/resource/1/jcpsa6/v139/i13/p134103_s1)
- [51] I. R. Craig, M. Thoss, H. Wang, Proton transfer reactions in model condensed-phase environments: Accurate quantum dynamics using the multilayer multiconfiguration time-dependent hartree approach, *J. Chem. Phys.* 127 (2007) 144503. doi:10.1063/1.2772265.
- [52] H. Wang, M. Thoss, Nonperturbative quantum simulation of time-resolved nonlinear spectra: Methodology and application to electron transfer reactions in the condensed phase, *Chem. Phys.* 347 (2008) 139–151, *ultrafast Photoinduced Processes in Polyatomic Molecules - Electronic Structure, Dynamics and Spectroscopy*. doi:DOI:10.1016/j.chemphys.2007.12.004.
- [53] Q. Meng, H.-D. Meyer, A multilayer MCTDH study on the full dimensional vibronic dynamics of naphthalene and anthracene cations, *J. Chem. Phys.* 138 (1) (2013) 014313. doi:10.1063/1.4772779.
- [54] M. F. Shibl, J. Schulze, M. J. Al-Marri, O. Kühn, Multilayer-MCTDH approach to the energy transfer dynamics in the LH2 antenna complex, *J. Phys. B: At., Mol. Opt. Phys.* 50 (2017) 184001. doi:10.1088/1361-6455/aa8374.
- [55] M. Brill, O. Vendrell, F. Gatti, H.-D. Meyer, *Shared Memory Parallelization of the Multi-Configuration Time-Dependent Hartree Method and Application to the Dynamics and Spectroscopy of the Protonated Water-Dimer*, Springer Berlin Heidelberg, Berlin, Heidelberg, 2008, pp. 141–155. doi:10.1007/978-3-540-74739-0\_10.
- [56] M. W. Schmidt, K. K. Baldridge, J. A. Boatz, S. T. Elbert, M. S. Gordon, J. H. Jensen, S. Koseki, N. Matsunaga, K. A. Nguyen, S. Su, T. L. Windus, M. Dupuis, J. A. Montgomery, General atomic and molecular electronic structure system, *J. Comput. Chem.* 14 (1993) 1347–1363. doi:10.1002/jcc.540141112.
- [57] W. J. Stevens, M. Krauss, H. Basch, P. G. Jasien, Relativistic compact effective potentials and efficient, shared-exponent basis sets for the third-, fourth-, and fifth-row atoms, *Can. J. Chem.* 70 (2) (1992) 612–630. doi:10.1139/v92-085.
- [58] R. J. Thompson, G. Rempe, H. J. Kimble, Observation of normal-mode splitting for an atom in an optical cavity, *Phys. Rev. Lett.* 68 (8) (1992) 1132–1135. doi:10.1103/physrevlett.68.1132.
- [59] S. M. Dutra, [Cavity Quantum Electrodynamics: The Strange Theory of Light in a Box](#), John Wiley & Sons, 2004. doi:10.1002/0471713465. URL <https://doi.org/10.1002/0471713465>
- [60] D. J. Tannor, *Introduction to quantum mechanics: a time-dependent perspective*, University Science Books, 2007.